PERGAMON

Solid State Communications 117 (2001) 649–954

solid state communications

www.elsevier.com/locate/ssc

InGaAs/GaAs quantum wells and quantum dots on (111)B orientation

S.L. Tyan[a,*], Y.G. Lin[a], F.Y. Tsai[b], C.P. Lee[b], P.A. Shields[c], R.J. Nicholas[c]

[a]*Department of Physics, National Cheng Kung University, Tainan, Taiwan, ROC*
[b]*Department of Electronics Engineering, National Chiao Tung University, Hsinchu, Taiwan, ROC*
[c]*Department of Physics, Clarendon Laboratory, University of Oxford, Parks Road, Oxford OX1 3PU, UK*

Received 3 November 1999; received in revised form 30 November 2000; accepted 15 December 2000 by P. Sheng

Abstract

We report a magneto optical characterization of InGaAs/GaAs quantum well (QW) and quantum dot (QD) structures grown on (111)B GaAs substrates. The photoluminescence (PL) peak shift under high excitation intensity is used to distinguish QW from QD structures together with atomic force microscopy (AFM) imaging. The binding energy in (111)InGaAs/GaAs QW is about 5 meV. The extent of the wave function obtained from the diamagnetic shift of the PL peak energy is consistent with the result calculated by the k.p method. The InGaAs/GaAs QD lateral confinement energy and the dot size are also estimated from the diamagnetic shift of the PL lines. The lateral confinement energy is estimated as 7 meV. The mean radius of the InGaAs QD is about 14 nm and the dot height is about 6 nm, which is in good agreement with the results as revealed in AFM imaging.

Keywords: A. Quantum wells; A. Nanostructures; D. Optical properties; E. Luminescence

PACS: 78.20.Ls

1. Introduction

Low-dimensional semiconductor microstructure such as quantum well (QW) has attracted much interest during the past decades, due both to the potential applications and to the interesting basic physics for opto-electronic devices. As a material for microelectronics and opto-electronics, InGaAs/GaAs QW structures have received attention due to the low effective mass of the carrier [1,2] and to the high optical gain [3]. Since semiconductor quantum dots (QDs) were suggested to improve the performance of opto-electronic device [4,5], there has been a variety of researches on fabrication techniques. The most popular method in QD fabrication is the Stranski–Krastanov (S–K) growth mode, utilizing strain relaxation between two materials with large lattice mismatch to facilitate the island growth. The fabrication of QDs using the S–K growth mode on (100) and (111)BGaAs substrates have been reported [6–8]. However, the control of growth conditions is critical for good uniformity of QDs. In our previous work [9], we had reported a simple method to fabricate high quality InGaAs/GaAs QDs on (111)BGaAs substrates by lowering the substrate temperature. The QW structure was grown at higher substrate temperature, while the QD structure fabricate, as the substrate temperature was lowered down. The formation of the QDs was identified by the atomic force microscopy (AFM) image.

Magneto-optics in high magnetic fields is a powerful tool to investigate the electronic states in low-dimensional systems. In this article, we report magneto-photoluminescence (PL) measurement on InGaAs/GaAs QW and QD structures on (111)B substrate. From the high excitation-intensity PL spectra, the structure of the sample could be categorized as QW or QD and is consistent with the results found in AFM images. The exciton binding energy deduced from the diamagnetic shift of the PL peak energy is about 5 meV. The k.p theory was employed in calculating the QW transition energy. The wave function calculated is consistent with that obtained from the diamagnetic shift of PL line. In

* Corresponding author. Tel.: +886-6-2088952; fax: +886-6-2747995.

E-mail address: sltyan@mail.ncku.edu.tw (S.L. Tyan).

0038-1098/01/$ - see front matter © 2001 Published by Elsevier Science Ltd.
PII: S0038-1098(01)00018-7

GaAs	50 nm
InGaAs	1.5 nm
GaAs	300 nm
(111)B GaAs Substrate	

Fig. 1. A schematic cross-section of the sample. All layers are undoped.

addition, the in-plane dot confinement energy and dot size are also estimated from the diamagnetic shift of the PL energy.

2. Experiment

A schematic cross-section of the sample is shown in Fig. 1. GaAs(111)B substrates with 2° off toward (211) were used. A GaAs buffer layer of 300 nm was first grown at a substrate temperature of 590°C. Next, a $In_{0.25}Ga_{0.75}As$ layer with a nominal thickness of 1.5 nm was grown. Before the growth of this layer, the substrate temperature was lowered during a growth interruption. Three different growth temperatures of 525, 515, 450°C were used for growing this layer. Samples A, B, and C correspond to these three growth conditions, respectively. Finally, a cap layer of 50 nm GaAs was grown. All layers were undoped. Samples A, B are QW structures, sample C can be identified as QD structure for small islands, revealed in the AFM image [9]. Another set of reference samples with the same structures but different substrate, GaAs(100), were grown simultaneously at each growth temperature.

Magneto-PL spectra were measured using an Oxford Instruments superconducting solenoid magnet system in field up to 15 T at 4.2 K in both Faraday ($B \parallel z$) and the

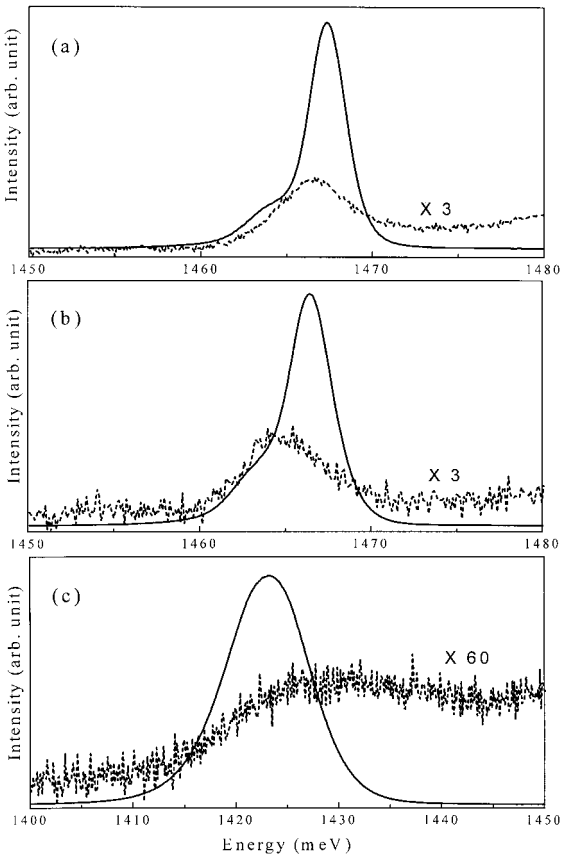

Fig. 2. PL spectra for samples A, B and C under low (solid lines) and high (dash lines) excitation intensity.

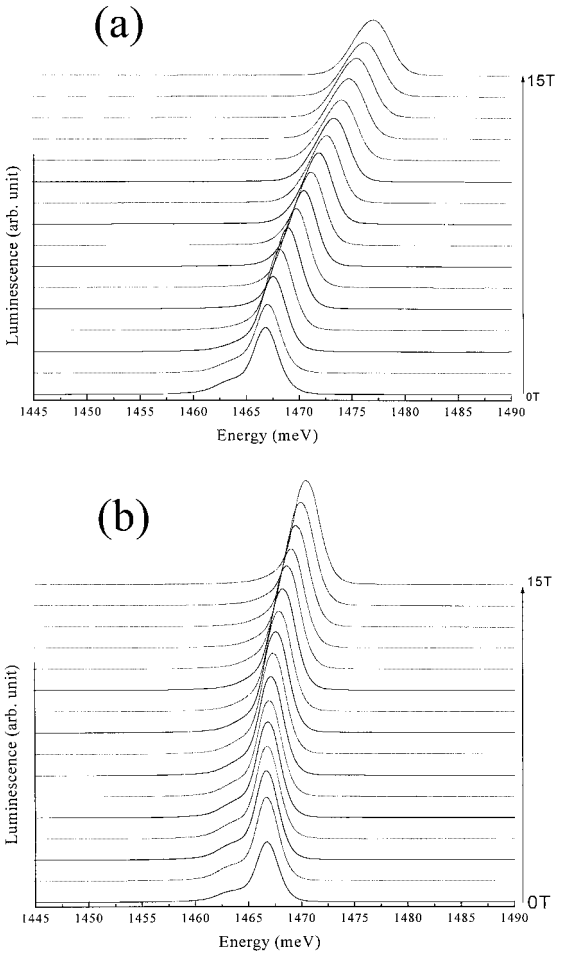

Fig. 3. The magneto-PL spectra in 1 T separation for sample A in (a) Faraday and (b) Voigt configurations.

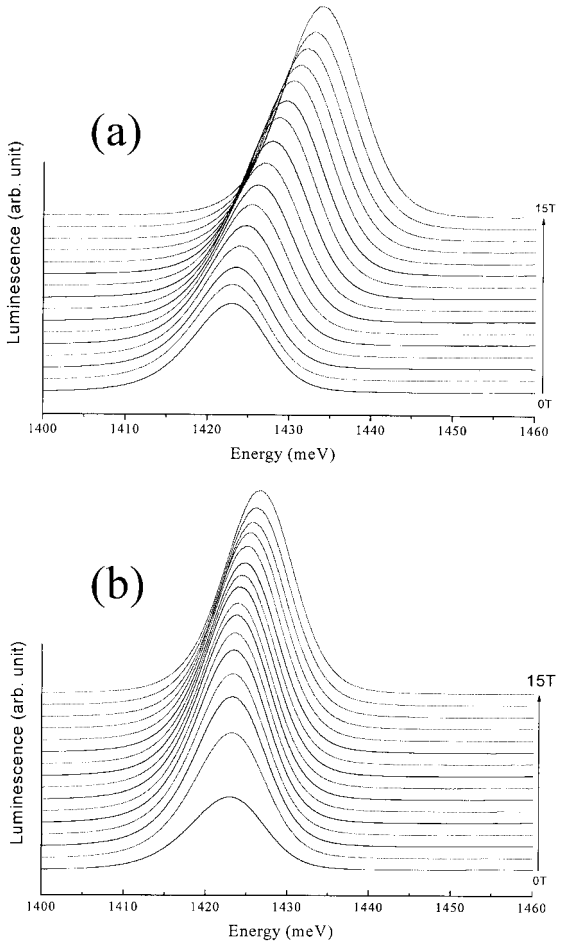

Fig. 4. The magneto-PL spectra in 1 T separation for sample C in (a) Faraday and (b) Voigt configurations.

Voigt configurations ($B \perp z$), where z denotes the growth direction. The PL spectra were obtained by a quarter meter spectrometer. The 690 nm line of a 10 mW solid laser is used for the illumination giving a maximum intensity of $\sim 10^{-2}$ W cm^{-2}. For the high intensity PL measurement, a 4 ns pulse laser emitting at $\lambda = 266$ nm at 10 Hz and with a maximum energy per pulse of 0.4 mJ was used, giving illumination intensities of 10^5 cm^{-2}.

3. Results and discussions

Fig. 2 shows the PL spectra for all samples measured under low CW (solid lines) and high (dash lines) pulsed excitation intensities at 4.2 K. The high power spectra were considerably noisier due to the low repetition rate (10 Hz) of the pulsed laser excitation. The transition energy, E_P, for low intensity pumping in the vicinity of 1467 meV in Fig. 2(a) results from exciton emission, the shoulder in the lower energy is probably due to an exciton bound to a neutral donor [10,11]. The half width at half maximum (HWHM) of the emission peak is about 2 meV, indicating the high quality of the sample. As the excitation intensity becomes higher, the peak broadens asymmetrically, and its maximum shifts to lower energy. This is due to the combined effect of high carrier-density-induced band-gap renormalization [12] and hot-carrier recombination [13] in QW. Fig. 2(b) shows a red shift under high excitation power as seen in Fig. 2(a), indicating the same quantum structure as sample A. The PL spectrum measured from sample C is shown in Fig. 2(c). The transition energy is about 1423 meV and the HWHM is 4.5 meV indicating excellent quality. On the contrary, the peak energy shifts to higher energy when the excitation intensity increased. The blue shift of the emission line is a clear indication of size quantization effect, which is caused by the inhomogeneous distribution of the dot sizes [14]. These spectra were another evidences in distinguishing the QW and QD structures and consistent with the results shown in the AFM image [9].

Fig. 3 shows the magneto-PL spectra in 1 T separation from QW sample A in both Faraday and Voigt configurations, respectively. Fig. 4 shows the magneto-PL spectra from QD sample C in both configurations. Both QW and QD peaks shift diamagnetically to the higher energy side, as the intensity of magnetic field increases. The shoulder of the peak in QW spectra disappears as the strength of magnetic field increases. Fig. 5 shows the diamagnetic shifts, ΔE, of the of the PL lines for all samples in both configurations. The peak positions were obtained from Gaussian lineshape fitting. The diamagnetic shifts in the Voigt configuration are smaller than that in the Faraday configuration because of the stronger confinement in the growth direction. In the low-field region of Faraday configuration, the field dependence of the PL shift is quadratic for the diamagnetic shift of the exciton. With increasing magnetic field, the peak energy shifts linearly, because the cyclotron energy associated with the magnetic field overcomes the Coulomb energy.

In order to obtain the exciton binding energy, E_b, in QW structure, the exciton reduced mass should be obtained at first. The heavy-hole effective mass for $In_{0.25}Ga_{0.75}As/GaAs$ QW in the (100) direction was determined as $0.23m_0$ (m_0 is the free electron mass) by extrapolation from values reported in previous articles [15–17]. Because the spin-splitting energy is much smaller than the fundamental transition energy and assumed that, the Kane matrix elements of InAs and GaAs are the same. The electron effective mass for $In_{0.25}Ga_{0.75}As/GaAs$ QW in the (100) direction can be estimated as $0.064m_0$ by Kane's theory [18] after the measured transition energy of the InGaAs QW is taken into account.

In QW structures, the wave functions of the electron and hole leak out far beyond the well because of the thin well width; therefore, a three-dimensional exciton model can be used to evaluate exciton binding energy. Fitting the low field

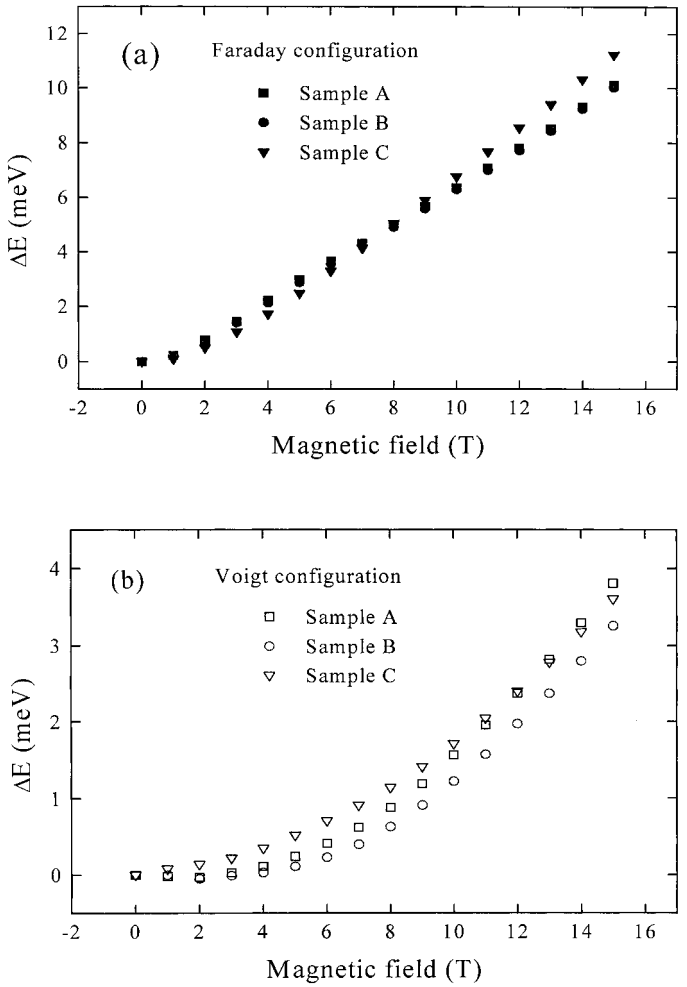

Fig. 5. The energy shifts of the PL lines, ΔE, for all samples in both configurations.

diamagnetic shift of the reference QW samples grown in (100) direction (not shown), to the numerical calculations of Makado [19] and using the exciton reduced mass $\mu_{100} = 0.050m_0$ obtained above, the binding energy can be deduced as ~7 meV. This value is in good agreement with the result of Moore et al. [16].

The exciton reduced mass, μ_{111}, for InGaAs/GaAs QW in the (111) direction, was obtained by the relation [20]

$$(\beta_{100}/\beta_{111})^{1/3} = \mu_{111}/\mu_{100}, \tag{1}$$

where β_{100} and β_{111} denote the diamagnetic shift coefficient in the (100) direction and the (111) direction, respectively. The value of μ_{111} was evaluated as $0.042m_0$ from Eq. (1). For the samples grown in the (111) direction and using the same method with $\mu_{111} = 0.042m_0$, the exciton binding energy for sample C is found to be smaller with a value of ~5 meV. The binding energy for the (111) direction growth is smaller than that for the (100) direction due to the internal electric fields, which tilt the confinement potentials and displace the confined wave functions, with the electron and hole states spatially localized at opposite sides of the well layers.

The transition energy at $B = 0$ can be calculated by

$$E_P = E_g + 11H - E_b, \tag{2}$$

where E_g and $11H$ are the band-gap, and the transition energy from the first conduction to the first valence subband of heavy hole character, respectively. We have used a 4-band k.p perturbation method to calculate the transition energy. There are two factors which should be considered: the strain effect produced by the high indium concentration and the internal piezoelectric field induced by non-zero diagonal components of the strain in the (111) orientation. The parameters are obtained by interpolation of InAs and GaAs [21] and the band-offset Q_v is 0.15 [22]. The transition energy calculated for a 15 Å well width is 1457 meV. This value is smaller than the observed value of 1467 meV. If the well width is reduced to 12 Å, agreement is found with the

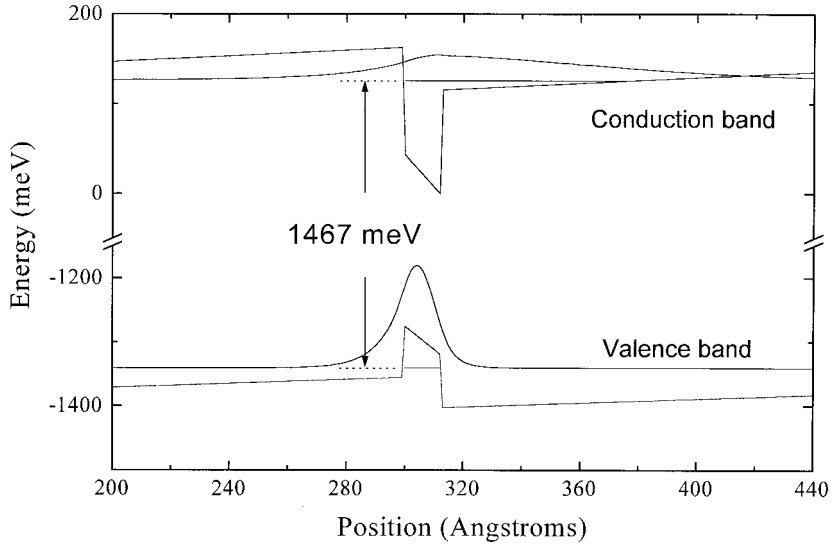

Fig. 6. The transition energy and wave functions of QW sample A calculated by k.p theory.

observed transition energy, as shown in Fig. 6. To a good approximation, it is reasonable to assign a well width of ~12 Å for QW samples.

The diamagnetic shift of the exciton peak at low field can be represented by [23,24]

$$\Delta E = (e^2\langle\rho^2\rangle/8\mu)B^2, \tag{3}$$

where $(\langle\rho^2\rangle)^{1/2}$ represents the extent of the confined wave function (ECWF) and the exciton reduced mass is assumed to be similar to that of previously used for (111) oriented structures. The diamagnetic coefficients for sample A are ~136 μeV T^{-2}, ~17 μeV T^{-2} for $B_{\|}$ and $B_{\perp}$, respectively. Using these values and Eq. (3), the in-plane ECWFs, $\langle\rho_x\rho_y\rangle^{1/2}$, then the ECWFs in z direction, $\langle\rho_z\rangle$, can be obtained as 16.2 and 2.1 nm, respectively, which is consistent with the results as shown in Fig. 6.

The diamagnetic coefficients for sample C are ~109 μeV T^{-2} and ~15 μeV T^{-2} for $B_{\|}$ and $B_{\perp}$, respectively. As mentioned above, we can use Eq. (3) to evaluate ECWFs. Using the values above gives $\langle\rho_x\rho_y\rangle \sim 208$ nm^2 for the area of the in-plane ECWF and $\langle\rho_x\rho_z\rangle \sim 31$ nm^2 for a cross-section through the dot. This suggests a mean dot radii of ~14 nm and an aspect ratio of ~0.15. This corresponds to a dot height of ~6 nm. The value is in good agreement with the result, 5 nm, obtained by AFM technique [9]. There will be considerable wave function penetration into the barrier for such a relatively weakly confined dot as studied here, and as a result the value is an overestimate relative to direct physical measurements such as AFM.

Assuming the in-plane confining potential of the dot is a parabolic potential

$$V = \tfrac{1}{2}\mu\omega_\rho^2\rho^2. \tag{4}$$

In the Faraday configuration, the ground state energy shift of the dot can be expressed as [25,26]

$$\Delta E = \tfrac{1}{2}\hbar\sqrt{\omega_c^2 + 4\omega_\rho^2}, \tag{5}$$

where $\omega_c = eB/\mu$ is the electron cyclotron frequency and $2\hbar\omega_\rho$ gives the in-plane dot confinement energy. By fitting the Eq. (5) to the experiment data, the lateral confinement energy can be estimated as $2\hbar\omega_\rho = 7$ meV. The confinement in the in-plane direction deduced is substantial but much less than that in the growth direction. The lateral size of the dot confined wave function is also consistent with the magnetic field at which the energy shift changes over to a linear increase in energy with field in the Faraday case. The confinement effects are negligible at this point and the cyclotron radius is approximately equal to the dot radius. Taking this field to be 4 T, the radius can be estimated as ~13 nm.

4. Conclusions

In conclusion, we have used high intensity PL measurements to confirm the structures of InGaAs layer grown in (111) direction at different temperatures. A red shift of the peak indicates a QW structure grown at high temperatures while a blue shift is found for QD structure grown at low temperature in agreement with the conclusions reached using AFM. The ECWF of the QW estimated from the excitonic diamagnetic shift is consistent with the results calculated by k.p theory. The exciton binding energy for InGaAs/GaAs QW in the (111) direction is about 5 meV. The InGaAs/GaAs QD lateral confinement energy and the dot size are estimated from the diamagnetic shift. The size of the dots deduced from magneto-PL is in agreement with the results of AFM.

Acknowledgements

This work was supported by the National Science Council of the Republic of China under Contract No. NSC89-2112-M006-038.

References

[1] D.C. Reynolds, K.R. Evans, K.K. Bajaj, B. Jogai, C.E. Stutz, P.W. Yu, Phys. Rev., B 43 (1991) 1871.
[2] J. Sanchez-Dehesa, J.L. Sanchez-Rojas, C. Lopez, R.J. Nicholas, Appl. Phys. Lett. 61 (1992) 1072.
[3] E. Fortin, B.Y. Hua, A.P. Roth, A. Charlebois, S. Fafard, C. Lacelle, J. Appl. Phys. 66 (1989) 4854.
[4] Y. Arakawa, H. Sakaki, Appl. Phys. Lett. 40 (1982) 939.
[5] H. Sakaki, Jpn. J. Appl. Phys. 49 (1986) 1043.
[6] D.I. Lubyshev, P.P. Gonzalez-Borrero, E. Marega Jr, E. Petitprez, N. La Scala Jr, P. Basmaji, Appl. Phys. Lett. 68 (1996) 205.
[7] D. Leonard, M. Krishnamurthy, C.M. Reaves, S.P. Denbaars, P.M. Petroff, Appl. Phys. Lett. 63 (1993) 3203.
[8] D.I. Lubyshev, P.P. Gonzalez-Borrero, E. Marega Jr, E. Petitprez, P. Basmaji, J. Vac. Sci. Technol., B 14 (1996) 2212.
[9] F.Y. Tsai, C.P. Lee, J. Appl. Phys. 84 (1998) 2624.
[10] A. Patane, A. Polimeni, M. Capizzi, F. Martelli, Phy. Rev., B 52 (1995) 2784.
[11] P.B. Kirby, J.A. Constable, R.S. Smith, Phys. Rev., B 40 (1989) 3013.
[12] S. Tarucha, H. Kobayashi, Y. Horikoshi, H. Okamoto, Jpn. J. Appl. Phys. 23 (1984) 874.
[13] D.S. Chemla, D.A.B. Miller, P.W. Smith, A.C. Gossard, W. Wieqmann, IEEE J. Quantum Electron. QE-20 (1984) 265.
[14] F. Daiminger, A. Schmidt, K. Pieger, F. Faller, A. Forchel, Semicond. Sci. Technol. 9 (1994) 896.
[15] N.J. Pulsford, R.J. Nicholas, R.J. Warburton, G. Duggan, K.J. Moore, K. Woodbridge, C. Roberts, Phys. Rev. B 43 (1991) 2246.
[16] K.J. Moore, G.D. Duggan, K. Woodbridge, C. Boberts, Phys. Rev. B 41 (1990) 1090.
[17] H.Q. Hou, Y. Segawa, Y. Aoyagi, S. Namba, J.M. Zhou, Phys. Rev. B 42 (1990) 1284.
[18] G. Bastard, J.A. Brum, R. Ferreira, in: H. Ehrenreich, D. Turnbull (Eds.), Solid State Physics, Vol. 44, Academic Press, New York, 1991, p. 234.
[19] P.C. Makado, Physica 132 B (1985) 7.
[20] S.H. Pan, H. Shen, Z. Hang, F.H. Pollak, W. Zhuang, Q. Xu, A.P. Roth, R.A. Masut, C. Lacelle, D. Morris, Phys. Rev. B 38 (1988) 3375.
[21] Landolt-Börnstein, in: O. Madelung (Ed.), Numerical Data and Functional Relationships in Science and Technology, New series group III, Vol. 22a, Springer, Berlin, 1987, p. 63 (see also p. 117).
[22] D.J. Arent, Phys. Rev. B 41 (1990) 9843.
[23] R.K. Hayden, K. Uchida, N. Miura, A. Polimeni, S.T. Stoddart, M. Henini, L. Eaves, P.C. Main, Phys. B 249 (1998) 262.
[24] R. Rinaldi, R. Mangino, R. Cingolani, H. Lipsanen, M. Sopanen, J. Tulkki, M. Brasken, J. Ahopelto, Phys. Rev. B 57 (1998) 9763.
[25] P.D. Wang, J.L. Mertz, S. Farad, R. Leon, D. Leonard, G. Medeiros-Ribeiro, M. Oestreich, P.M. Petroff, K. Uchida, N. Miura, H. Akiyama, H. Sakaki, Phys. Rev. B 53 (1996) 16458.
[26] G. Bastard, Wave Mechanics Applied to Semiconductor Heterostructures, les editions de physique, Les Ulis, 1996, pp. 317–325.